The Astronomical Journal, 162:41 (9pp), 2021 August https://doi.org/10.3847/1538-3881/ac00bd


# Speckle Interferometry at SOAR in 2020

Andrei Tokovinin[1], Brian D. Mason[2], Rene A. Mendez[3], Edgardo Costa[3], Andrew W. Mann[4], and Todd J. Henry[5]
[1] Cerro Tololo Inter-American Observatory—NFSs NOIRLab Casilla 603, La Serena, Chile; andrei.tokovinin@noirlab.edu
[2] U.S. Naval Observatory, 3450 Massachusetts Avenue, Washington, DC, USA; brian.d.mason.civ@mail.mil
[3] Universidad de Chile, Casilla 36-D, Santiago, Chile; rmendez@uchile.cl
[4] Department of Physics and Astronomy, University of North Carolina at Chapel Hill, Chapel Hill, NC 27599-3255, USA
[5] RECONS Institute, Chambersburg, PA 17201, USA
*Received 2021 April 11; revised 2021 May 8; accepted 2021 May 11; published 2021 July 2*

## Abstract

The results of speckle interferometric observations at the 4.1 m Southern Astrophysical Research Telescope in 2020, as well as earlier unpublished data, are given, totaling 1735 measurements of 1288 resolved pairs and nonresolutions of 1177 targets. We resolved for the first time 59 new pairs or subsystems in known binaries, mostly among nearby dwarf stars. This work continues our long-term speckle program. Its main goal is to monitor orbital motion of close binaries, including members of high-order hierarchies and Hipparcos pairs in the solar neighborhood. We also report observations of 892 members of young moving groups and associations, where we resolved 103 new pairs.

*Unified Astronomy Thesaurus concepts:* Binary stars (154); Multiple stars (1081); Stellar associations (1582)

*Supporting material:* machine-readable tables

## 1. Introduction

This paper continues the series of double-star measurements made at the 4.1 m Southern Astrophysical Research Telescope (SOAR) with the speckle camera, HRCam. Previous results were published in Tokovinin et al. (2010a, hereafter TMH10; and in Tokovinin et al. 2010b; Hartkopf et al. 2012; Tokovinin 2012; Tokovinin et al. 2014, 2015, 2016, 2018, 2019, 2020). Observations were made during 2020, but this work also includes earlier unpublished observations.

The structure and content of this paper are similar to other papers of this series. Section 2 reviews all speckle programs that contributed to this paper, the observing procedure, and the data reduction. The results are presented in Section 3 in the form of electronic tables archived by the journal. We also discuss new resolutions and new orbits resulting from this data set. A short summary in Section 4 concludes the paper.

## 2. Observations

### 2.1. Observing Programs

As in previous years, HRCam (see Section 2.2) was used during 2020 to execute several observing programs, some with common targets. Table 1 gives an overview of these programs and indicates which observations are published in the present paper. The numbers of observations are approximate. Overall, 2348 observations were made during 2020. Here is a brief description of these programs.

*Orbits* of resolved binaries. New measurements contribute to the steady improvement of the quantity and quality of orbits in the Sixth Catalog of Visual Binary Star Orbits (Hartkopf et al. 2001). See Mendez et al. (2021) for an example of this work.

*Hierarchical systems* of stars are of special interest because their architecture is relevant to star formation, while dynamical evolution of these hierarchies increases chances of stellar interactions and mergers (Toonen et al. 2020). We followed orbital motions of several triple systems and used these data for orbit determinations (Tokovinin & Latham 2020; Tokovinin 2020, 2021a). Some observations made in 2020 were published in the above papers. They are duplicated here to provide a complete and homogeneous record of the SOAR speckle data.

*Hipparcos binaries* within 200 pc are monitored to measure masses of stars and to test stellar models, as outlined by, e.g., Horch et al. (2015, 2017, 2019). The southern part of this sample is addressed at SOAR (Mendez et al. 2017). This program overlaps with the general work on visual orbits.

*Neglected close binaries* from the Washington Double Star Catalog (WDS; Mason et al. 2001) were observed as a "filler" at low priority. In some cases, we resolved new inner subsystems, thus converting classical visual pairs into hierarchical triples. Some WDS pairs are moving fast near periastron, allowing calculation of their first orbits after several observations at SOAR.

*Nearby K and M dwarfs* were observed since 2018 on the initiative of T. Henry and E. Vrijmoet. The goal is to assemble statistical data on orbital elements, focusing on short periods. The sample includes known and suspected binaries detected by astrometric monitoring, Gaia, etc. Data on M dwarfs are being published by E. Vrijmoet et al. (2021, in preparation), while observations of K dwarfs are reported here.

*TESS follow-up* received a substantial time allocation in 2020, continuing the program of 2018–2019. Its first results are published by Ziegler et al. (2020), the paper with additional data is submitted (Ziegler et al. 2021). All speckle observations of TESS targets of interest are promptly posted on the EXOFOP website. These data are used in the growing number of papers on TESS exoplanets, mostly as limits on potential companions to exohosts.

*Young moving groups and associations* were selected as part of a program aimed at characterizing planets and young stellar associations with TESS (the THYME survey; Newton et al. 2019). These sources were selected because they have been observed by TESS and are likely to be young or members of nearby stellar associations reported in the literature. The majority of stars (549) were drawn from the BANYAN survey of young moving groups within 150 pc (Gagné et al. 2018), as well as 82 members of the Scorpius–Centaurus (Sco-Cen) OB

**Table 1**
Observing Programs

| Program | PI | *N* | Publ.[a] |
|---|---|---|---|
| Orbits | Mason, Tokovinin | 562 | Yes |
| Hierarchical systems | Tokovinin | 82 | Yes |
| Hipparcos binaries | Mendez, Horch | 267 | Yes |
| Neglected binaries | R. Gould, Tokovinin | 152 | Yes |
| Nearby K dwarfs | T. Henry | 228 | Yes |
| Nearby M dwarfs | E. Vrijmoet | 354 | No |
| TESS follow-up | C. Ziegler | 355 | No |
| Young moving groups | A. Mann | 985 | Yes |
| Stars with RV trends | B. Pantoja | 195 | Yes |

**Note.**
[a] This columns indicates whether the results are published here (Yes) or deferred to future papers (No).

association (Sco-Cen) from Rizzuto et al. (2015) excluding those already surveyed by Tokovinin & Briceño (2020) and 261 suspected pre-main-sequence stars within 500 pc from Zari et al. (2018). For both BANYAN and Sco-Cen members, membership for targets were determined primarily using Bayesian membership probabilities based on kinematics of each star and the association using Gaia DR2 astrometry. Sources from Zari et al. (2018) were selected based on their elevated position relative to the main sequence on a color–magnitude diagram. Because all target selection relied on Gaia DR2, any systematics present in the Gaia catalog (e.g., missing binaries) will be present in the targets surveyed here. The names of these objects in the data tables begin by "*T*" followed by their number in the TESS input catalog (TIC; Stassun et al. 2019).

*Stars with radial velocity trends* have been monitored since 2016 on request from B. Pantoja, with the aim to resolve potential companions causing these trends (e.g., Pantoja et al. 2018). Five new pairs and one triple (GJ 3260) were resolved at SOAR and measured during five years.

If observations of a given star were requested by several programs, they are published here even if the other program is still ongoing. We also publish here the measurements of previously known pairs resolved during surveys, for example, in the TESS follow-up.

### 2.2. Instrument and Observing Procedure

The observations reported here were obtained with the high-resolution camera (HRCam)—a fast imager designed to work at the 4.1 m SOAR telescope (Tokovinin 2018). The instrument and observing procedure were described in the previous papers of this series (e.g., Tokovinin et al. 2020), so only the basic facts are included here. We used mostly the near-infrared *I* filter (824/170 nm) and the Strömgren *y* filter (543/22 nm), with a few observations made in the *B*, *V*, and *R* filters; the transmission curves of HRCam filters are given in the instrument manual. In the standard observing mode, two series of 400 200 × 200 pixel images (image cubes) are recorded. The pixel scale is 0.″01575, hence the field of view is 3.″15; the exposure time is normally 24 ms. For survey programs such as TESS follow-up, we use the *I* filter and a 2 × 2 binning, doubling the field. Pairs wider than ∼1.″4 are observed with a 400 × 400 pixel field, and the widest pairs are sometimes recorded with the full field of 1024 pixels (16″) and a 2 × 2 binning.

The speckle power spectra are calculated and displayed immediately after the acquisition for quick evaluation of the results. Observations of close pairs are accompanied by observations of single (reference) stars to account for such instrumental effects as telescope vibration or aberrations. Bright stars can be resolved and measured below the formal diffraction limit by fitting a model to the power spectrum and using the reference. The resolution and contrast limits of HRCam are further discussed in TMH10 and in the previous papers of this series.

A custom software helps to optimize observations by selecting targets, pointing the telescope, and logging. Typically, about 300 targets are covered on a clear night. The observing programs are executed in an optimized way, depending on the target visibility, atmospheric conditions, and priorities, while minimizing the telescope slews. Reference stars and calibrator binaries are observed alongside the main targets as needed.

During 2020, the SOAR telescope was closed from March 18 to October 7 due to COVID-19 pandemic. The number of observations obtained in 2020, 2348, is less than in 2018 and 2019. The sporadic telescope vibration that affected HRCam observations previously (see Section 3.5 in Tokovinin 2018) was much less frequent in 2020.

### 2.3. Data Processing and Calibration

The data processing is described in TMH10 and Tokovinin (2018). We use the standard speckle interferometry technique based on the calculation of the power spectrum and the speckle auto-correlation function (ACF). Companions are detected as secondary peaks in the ACF and/or as fringes in the power spectrum. Parameters of the binary and triple stars (separation $\rho$, position angle $\theta$, and magnitude difference $\Delta m$) are determined by modeling (fitting) the observed power spectrum. The true quadrant is found from the shift-and-add (SAA) images whenever possible because the standard speckle interferometry determines position angles modulo 180°.

The pixel scale and angular offset are inferred from observations of several relatively wide (from 0.″5 to 3″) calibration binaries. Their motion is accurately modeled based on previous observations at SOAR. The models are adjusted iteratively (the latest adjustment in 2019 November). Measurements of those wide calibrators by Gaia (Gaia Collaboration et al. 2018) show very small systematic errors of these models (Tokovinin et al. 2019). Typical rms deviations of the observations of calibrators from their models are 0.°2 in angle and 1 to 3 mas in separation. The astrometric accuracy strongly depends on the target characteristics (larger errors at large $\Delta m$ and for faint pairs), as well as on the seeing and telescope vibration. The contrast limit for companion detection also depends on the conditions, so that difficult pairs can be resolved in one observing run and unresolved in another run.

## 3. Results

### 3.1. Data Tables

The results (measures of resolved pairs and nonresolutions) are presented in exactly the same format as in Tokovinin et al. (2020). The long tables are published electronically; here we describe their content.

Table 2 lists 1735 measures of 1288 resolved pairs and subsystems, including new discoveries. The pairs are identified

**Table 2**
Measurements of Double Stars at SOAR

| Col. | Label | Format | Description, Units |
|---|---|---|---|
| 1 | WDS | A10 | WDS code (J2000) |
| 2 | Discov. | A16 | Discoverer code |
| 3 | Other | A12 | Alternative name |
| 4 | R.A. | F8.4 | R.A. J2000 (deg) |
| 5 | Decl. | F8.4 | decl. J2000 (deg) |
| 6 | Epoch | F9.4 | Julian year (yr) |
| 7 | Filt. | A2 | Filter |
| 8 | $N$ | I2 | Number of averaged cubes |
| 9 | $\theta$ | F8.1 | Position angle (deg) |
| 10 | $\rho\sigma_\theta$ | F5.1 | Tangential error (mas) |
| 11 | $\rho$ | F8.4 | Separation (arcsec) |
| 12 | $\sigma_\rho$ | F5.1 | Radial error (mas) |
| 13 | $\Delta m$ | F7.1 | Magnitude difference (mag) |
| 14 | Flag | A1 | Flag of magnitude difference[a] |
| 15 | $(O-C)_\theta$ | F8.1 | Residual in angle (deg) |
| 16 | $(O-C)_\rho$ | F8.3 | Residual in separation (arcsec) |
| 17 | Ref. | A8 | Orbit reference[b] |

**Notes.**
[a] Flags: $q$—the quadrant is determined; *—$\Delta m$ and quadrant from average image; :—noisy data or tentative measures.
[b] References are provided at https://www.astro.gsu.edu/wds/orb6/wdsref.txt.

(This table is available in its entirety in machine-readable form.)

by their WDS-style codes based on the J2000 coordinates and discoverer designations adopted in the WDS catalog (Mason et al. 2001), as well as by alternative names in column (3), mostly from the Hipparcos catalog. Equatorial coordinates for the epoch J2000 in degrees are given in columns (4) and (5) to facilitate matching with other catalogs and databases. In the case of resolved multiple systems, the position measurements and their errors (columns 9–12) and magnitude differences (column 13) refer to the individual pairings between components, not to their photocenters. As in the previous papers of this series, we list the internal errors derived from the power spectrum model and from the difference between the measures obtained from two data cubes. The real errors are usually larger, especially for difficult pairs with substantial $\Delta m$ and/or with small separations. Residuals from orbits and from the models of calibrators, typically between 1 and 5 mas rms, characterize the external errors of the HRcam astrometry.

The flags in column (14) indicate the cases where the true quadrant is determined (otherwise the position angle is measured modulo 180°), when the relative photometry of wide pairs is derived from the long-exposure images (this reduces the bias caused by speckle anisoplanatism), and when the data are noisy or the resolutions are tentative (see TMH10). For binary stars with known orbits, the residuals to the latest orbit and its reference are provided in columns (15)–(17).

Nonresolutions are reported in Table 3. Its first columns (1)–(8) have the same meaning and format as in Table 2. Column (9) gives the minimum resolvable separation when pairs with $\Delta m < 1$ mag are detectable. It is computed from the maximum spatial frequency of the useful signal in the power spectrum and is normally close to the formal diffraction limit $\lambda/D$. The following columns (10) and (11) provide the indicative dynamic range, i.e., the maximum magnitude difference at separations of 0.″15 and 1″, respectively, at the 5$\sigma$ detection level. The last column (12) marks noisy data by the flag ":".

Table 2 contains 162 pairs resolved for the first time; some of those were confirmed in subsequent observing runs. In the following subsections we discuss the new pairs.

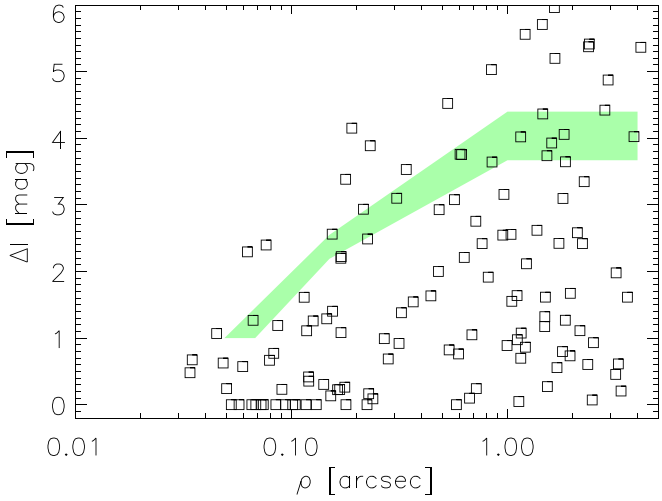


**Figure 1.** Resolved pairs in the YMG sample: $\Delta I$ vs. separation. The shaded green area depicts the lower and upper quartiles of the detection limits.

**Table 3**
Unresolved Stars

| Col. | Label | Format | Description, Units |
|---|---|---|---|
| 1 | WDS | A10 | WDS code (J2000) |
| 2 | Discov. | A16 | Discoverer code |
| 3 | Other | A12 | Alternative name |
| 4 | R.A. | F8.4 | R.A. J2000 (deg) |
| 5 | Decl. | F8.4 | decl. J2000 (deg) |
| 6 | Epoch | F9.4 | Julian year (yr) |
| 7 | Filt. | A2 | Filter |
| 8 | $N$ | I2 | Number of averaged cubes |
| 9 | $\rho_{\min}$ | F7.3 | Angular resolution (arcsec) |
| 10 | $\Delta m(0.15)$ | F7.2 | Max. $\Delta m$ at 0.″15 (mag) |
| 11 | $\Delta m(1)$ | F7.2 | Max. $\Delta m$ at 1″ (mag) |
| 12 | Flag | A1 | : marks noisy data |

(This table is available in its entirety in machine-readable form.)

### 3.2. Young Moving Groups and Associations

The TESS follow-up program started in 2018. It was complemented by a sample of the members of young moving groups and associations (YMGs) based on the TESS input catalog, TIC (Stassun et al. 2019), and Gaia astrometry. These objects are identified here by TIC numbers preceded by the letter "$T$". Overall, 892 objects from this program were observed at least once. The largest number of observations (608) were secured in 2019, and only 32 in 2020; the total number of observations is 985 (some newly resolved pairs were revisited).

Figure 1 plots the magnitude difference $\Delta I$ versus separation $\rho$ for resolved pairs of the YMG sample. One notes the paucity of pairs with separations from 0.″2 to 0.″7 and a small $\Delta I$. Such near-equal pairs do not have astrometry in Gaia and, for this reason, were not included in the sample, which is, therefore, biased against such binaries.

**Table 4**
New YMG Pairs

| WDS | TIC | $\rho$ (arcsec) | $\Delta I$ (mag) | $N$[a] |
|---|---|---|---|---|
| 00376−2709 | 246895416 | 0.14 | 2.5 | 4 |
| 02002−8025 | 273789976 | 0.03 | 0.0 | 3 |
| 02109−4604 | 7242537 | 0.21 | 2.9 | 2 |
| 02489−3404 | 122671519 | 0.05 | 0.0 | 2 |
| 02568−6343 | 220556639 | 0.07 | 0.0 | 3 |
| 03165−3541 | 176832633 | 0.19 | 4.4 | 3 |
| 03259−3556 | 142874733 | 0.06 | 2.3 | 3 |
| 04001−2902 | 44670258 | 0.07 | 2.4 | 1? |
| 04084−2745 | 44793998 | 0.37 | 1.5 | 2 |
| 04316−3043 | 170699229 | 0.44 | 1.6 | 1 |
| 04536−2836 | 671393 | 0.13 | 0.0 | 2 |
| 05085−2102 | 146539195 | 0.05 | 0.6 | 3 |
| 05287−3327 | 24448282 | 0.14 | 1.2 | 2 |
| 05371−3932 | 144499196 | 0.16 | 1.3 | 2 |
| 05412−4118 | 21438160 | 0.07 | 0.0 | 3 |
| 05425−1535 | 46739994 | 1.15 | 0.7 | 1 |
| 05471−3211 | 100608178 | 0.27 | 1.0 | 1 |
| 05473−5450 | 350563576 | 0.84 | 5.0 | 1 |
| 05504−2915 | 32930236 | 0.85 | 3.6 | 1 |
| 05597−6209 | 149935360 | 1.15 | 4.0 | 1 |
| 06086−3403 | 201391310 | 0.57 | 3.1 | 1 |
| 06086−5704 | 260127241 | 0.12 | 0.0 | 1 |
| 06220−7932 | 270424741 | 0.06 | 0.0 | 1 |
| 06462−8359 | 397231463 | 1.45 | 5.7 | 1 |
| 07019−3922 | 157212164 | 1.83 | 4.1 | 1 |
| 07147−4010 | 22766740 | 0.16 | 0.1 | 2 |
| 07310−8419 | 405077613 | 0.61 | 3.8 | 1 |
| 07336−4019 | 173957127 | 1.70 | −0.15 | 1* |
| 07336−4019 | 173957127 | 0.12 | 0.6 | 1* |
| 07406−6704 | 300741570 | 2.27 | 3.4 | 1 |
| 07418−4630 | 123642034 | 1.49 | 1.2 | 1 |
| 07437−6107 | 281582156 | 0.18 | 3.4 | 2 |
| 07571−2227 | 142844055 | 1.16 | 1.1 | 1 |
| 08262−3902 | 183974196 | 0.24 | 0.1 | 1 |
| 09095−5538 | 385012516 | 0.05 | 0.1 | 4 |
| 10054−7137 | 372515598 | 0.10 | 0.0 | 2 |
| 10056−5731 | 462492721 | 3.85 | 4.0 | 1 |
| 10074−4622 | 311258541 | 0.18 | 0.1 | 2 |
| 10207−6311 | 378126824 | 0.32 | 1.4 | 2 |
| 10330−6144 | 460604193 | 0.52 | 4.5 | 1 |
| 11081−6342 | 466799461 | 2.37 | 5.4 | 1 |
| 11098−3828 | 151738485 | 0.05 | 1.1 | 1? |
| 11099−3739 | 151762498 | 0.06 | 0.6 | 1 |
| 11262−5823 | 451452509 | 0.11 | 1.6 | 1 |
| 11545−5325 | 400913139 | 0.03 | 0.7 | 1? |
| 12172−1033 | 203233128 | 0.12 | 0.4 | 1 |
| 12269−3316 | 130722957 | 0.67 | 0.1 | 1 |
| 12328−7654 | 360339486 | 0.17 | 1.0 | 2 |
| 12559−7417 | 361525866 | 1.10 | 0.7 | 2 |
| 12577−6652 | 335287811 | 0.13 | 0.3 | 3 |
| 13090−5720 | 253501247 | 4.10 | 0.9 | 1 |
| 13123−5441 | 406376573 | 1.00 | 0.9 | 1 |
| 13137−5807 | 406694754 | 0.68 | 1.0 | 2 |
| 13260−5112 | 438733975 | 0.11 | 1.1 | 3 |
| 13271−4856 | 438790187 | 0.95 | 2.5 | 2 |
| 13275−4719 | 438627800 | 2.82 | 4.4 | 1 |
| 13341−5624 | 457308993 | 1.12 | 0.1 | 1* |
| 13341−5624 | 457308993 | 0.09 | 0.0 | 1* |
| 13413−4537 | 243415454 | 3.59 | 1.6 | 1 |
| 13415−4431 | 243425206 | 2.47 | 0.0 | 1* |
| 13415−4431 | 243425206 | 0.66 | 0.1 | 1* |
| 13453−4102 | 166302995 | 0.31 | 3.1 | 1 |
| 13485−6727 | 429383724 | 0.71 | 2.8 | 1 |
| 13491−4413 | 243621789 | 2.92 | 4.9 | 1 |
| 13523−3826 | 166624597 | 0.13 | 1.3 | 1 |
| 13538−5502 | 208387087 | 3.17 | 0.5 | 1 |
| 13579−4432 | 359830202 | 0.17 | 2.2 | 1 |
| 14028−1850 | 6119516 | 1.80 | 0.8 | 1 |
| 14161−4031 | 179793360 | 0.17 | 2.2 | 2 |
| 14169−3648 | 179819049 | 0.08 | 0.0 | 1 |
| 14171−4038 | 179829109 | 0.96 | 3.2 | 1 |
| 14241−3923 | 167542104 | 1.50 | 1.6 | 1 |
| 14381−4322 | 128453434 | 1.11 | 1.6 | 1 |
| 14463−5056 | 250091359 | 0.63 | 2.2 | 1 |
| 14535−3903 | 160451137 | 1.04 | 2.6 | 1 |
| 14541−3606 | 160574439 | 0.08 | 0.8 | 1 |
| 14544−3718 | 160576551 | 3.26 | 0.6 | 1 |
| 14592−4012 | 121196256 | 2.50 | 0.9 | 1 |
| 15180−3335 | 272248916 | 0.08 | 0.0 | 2 |
| 15206−3132 | 460325085 | 1.22 | 2.1 | 1 |
| 15230−3052 | 54077774 | 2.17 | 0.6 | 1* |
| 15230−3052 | 54077774 | 0.36 | 1.1 | 1* |
| 15233−3127 | 54077130 | 3.35 | 0.2 | 1 |
| 15280−3208 | 54512674 | 2.22 | 2.4 | 1 |
| 15299−3136 | 54667962 | 1.73 | 2.4 | 1 |
| 15312−3505 | 54802536 | 0.08 | 0.7 | 2 |
| 15476−3127 | 442571495 | 0.07 | 0.0 | 1 |
| 16186−3839 | 318141352 | 1.66 | 5.2 | 1 |
| 16210−0617 | 135890809 | 0.05 | 0.2 | 1 |
| 16223−3843 | 4061225 | 0.81 | 1.9 | 1 |
| 16338−5119 | 22836043 | 1.81 | 3.1 | 1* |
| 16338−5119 | 22836043 | 0.13 | 1.1 | 1* |
| 16345−1106 | 152667565 | 1.95 | 0.7 | 1 |
| 16361−1324 | 414338264 | 1.21 | 5.6 | 1 |
| 16498−1239 | 398869084 | 0.60 | 3.8 | 1 |
| 16502−1108 | 181292505 | 0.76 | 2.4 | 1 |
| 17076−0515 | 142638811 | 0.23 | 2.5 | 1 |
| 17123−1131 | 146003265 | 0.09 | 0.0 | 1 |
| 17142−0038 | 176322832 | 0.48 | 2.9 | 1 |
| 17185−7858 | 384747990 | 0.12 | 0.4 | 1 |
| 17563−5833 | 337276808 | 1.85 | 1.3 | 1 |
| 20108−3845 | 269768590 | 1.37 | 2.6 | 2 |
| 20146−5431 | 201751726 | 0.58 | 0.0 | 1 |
| 21123−8129 | 403995704 | 0.10 | 0.0 | 1 |
| 21210−5229 | 79403459 | 0.09 | 0.2 | 4 |
| 21215−6655 | 419610508 | 0.06 | 1.3 | 1 |
| 21589−4706 | 389726031 | 0.15 | 0.0 | 3 |

**Note.**
[a] The question mark indicates unreliable resolutions; asterisks distinguish triple stars.

There are 129 resolved pairs among 892 YMG objects, so the observed raw multiplicity rate is 14.5%. Most of these pairs (103) are new discoveries. Statistical analysis of the multiplicity is outside the scope of this paper, which only reports the observations. Some companions, especially those with large $\rho$ and $\Delta I$, can be unrelated stars (optical pairs). All newly resolved YMG pairs are listed in Table 4. They are identified by the WDS-style code and the TIC numbers. The following columns contain the separation $\rho$, the magnitude difference $\Delta I$, and the number of visits $N$ where the pair was resolved. Mostly, we revisited close pairs and found that some of them show

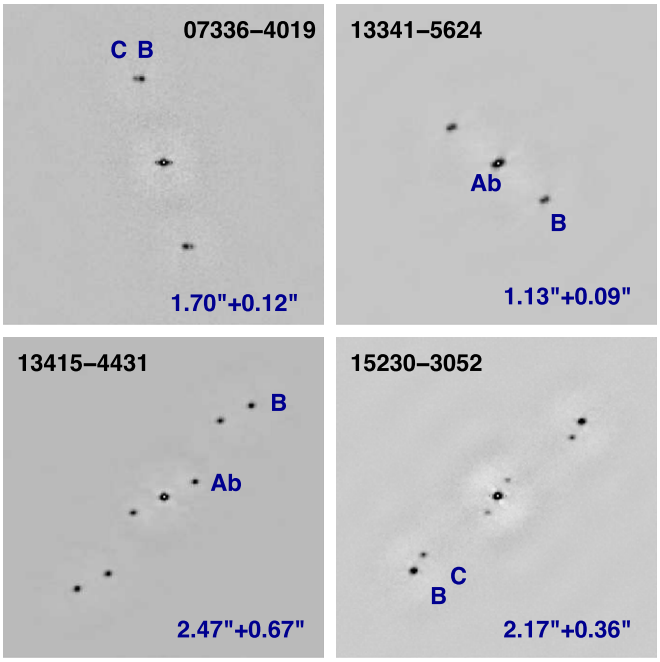


**Figure 2.** Four new triples in the YMG sample. The panels show speckle ACFs (in negative rendering) in the full 3.″15 field. The letters mark secondary peaks corresponding to the companions (as opposed to the mirror peaks) inferred from the SAA images. The separations of the outer and inner pairs in arcseconds are given in the lower right corner.

rapid orbital motion on the time span of 1–3 yr. They are promising candidates for future orbit determinations and measurements of masses. Three new close pairs were not resolved in subsequent visits either because they moved under the resolution limit or because the first resolutions were unreliable. These stars can be in fact single; they are distinguished by question marks in the last column, and further observations are needed to confirm these pairs.

The resolution and contrast limits depend on the seeing and target magnitude. One might think that brighter targets have a larger chance of binary detection. However, the median TESS magnitudes $T$ of the resolved and unresolved targets are 11.4 and 11.5 mag, respectively, and their distributions look alike. Therefore, the magnitude bias is small, if any. The total range of magnitudes in this sample is from $T = 6$ to $T = 13$ mag.

Five YMG targets turned out to be resolved triple stars. They have two entries in Table 4 (one per subsystem), marked by asterisks in the last column. Figure 2 illustrates the ACFs of four new young triples out of five.

### 3.3. Other New Pairs

Table 5 highlights 59 pairs resolved in 2020 or resolved earlier but not yet published. All measurements of these pairs are found in Table 2. Table 5 is similar to Table 4, but it contains an additional column specifying the program. The largest number of new pairs, 36, comes from the survey of K-type dwarfs. Most of these were observed more than once, and some (the closest) are in rapid orbital motion. The combined spectro-interferometric orbit of one such pair, HIP 57058, is determined (Figure 4). Five pairs are serendipitous resolutions of reference stars (three of those predate 2020 but were not reported previously), two are new close subsystems in classical visual binaries (WDS program), and three are subsystems in multiple stars (MSC). Most new pairs

**Table 5**
New Double Stars

| WDS | Name | $\rho$ (arcsec) | $\Delta m$ (mag) | $N$ | Prog.[a] |
|---|---|---|---|---|---|
| 00111+0513 | HIP 898 | 0.12 | 2.5 | 2 | NKD |
| 01027−2519 | HIP 4874 | 0.10 | 3.4 | 6 | NKD |
| 01262+1349 | HIP 6705 | 0.79 | 3.6 | 2 | NKD |
| 01406+0846 | HIP 7819 | 0.09 | 1.3 | 2 | REF |
| 02035−0455 | HIP 9603 | 0.20 | 2.9 | 4 | NKD |
| 02324+0323 | HIP 11815 | 1.50 | 3.1 | 2 | NKD |
| 03225+1744 | HIP 15724 | 1.70 | 7.4 | 2 | NKD |
| 04007−2305 | GJ 3260AB | 1.35 | 2.6 | 7 | Pan |
| 04007−2305 | GJ 3260BC | 0.33 | 0.1 | 7 | Pan |
| 04141−3155 | TIC168789840 | 0.42 | 0.3 | 4 | TESS |
| 04234+1546 | HIP 20485 | 1.20 | 4.5 | 2 | NKD |
| 04279+2427 | HIP 20834 | 0.17 | 2.7 | 4 | NKD |
| 04330−1633 | HIP 21222 | 0.09 | 1.7 | 7 | NKD |
| 04518+1339 | BU 552Ba,Bb | 0.04 | 1.2 | 2 | MSC |
| 06006−5806 | HIP 28464 | 0.44 | 4.5 | 2 | REF |
| 06215+1718 | HIP 30220 | 0.92 | 3.0 | 3 | NKD |
| 06443−2349 | TDS4085BC | 0.33 | 0.4 | 1 | TESS |
| 07151+1556 | HIP 35071 | 1.10 | 2.6 | 2 | NKD |
| 07390+1913 | HIP 37246 | 0.44 | 1.4 | 3 | NKD |
| 07584−1501 | HIP 38969 | 0.11 | 3.1 | 2 | NKD |
| 08155+0959 | HIP 40449 | 0.23 | 0.1 | 3 | NKD |
| 08187−1512 | HIP 40724 | 0.07 | 2.3 | 8 | NKD |
| 08253+0415 | HIP 41277 | 0.35 | 3.7 | 3 | NKD |
| 08430+2408 | TOK 265Aa,Ab | 0.18 | 2.2 | 4 | NKD |
| 09095−0024 | HIP 44953 | 1.38 | 3.7 | 2 | NKD |
| 09308+1815 | HIP 46662 | 0.14 | 2.7 | 5 | NKD |
| 09361−5145 | RST 415Aa,Ab | 0.14 | 1.7 | 1 | TESS |
| 09380+2231 | HIP 47261 | 1.11 | 3.7 | 2 | NKD |
| 09429−5502 | RST3660Aa,Ab | 0.07 | 1.3 | 3 | WDS |
| 09527−7933 | KOH 86Aa,Ab | 0.04 | 1.7 | 1 | MSC |
| 10041+1848 | HIP 49324 | 0.13 | 0.1 | 6 | NKD |
| 10211−1744 | HIP 50696 | 0.59 | 1.2 | 3 | NKD |
| 10212−5143 | I 853Ba,Bb | 0.09 | 1.0 | 3 | WDS |
| 10262−6318 | HIP 51083 | 0.10 | 2.5 | 2 | REF |
| 10283−2416 | HIP 51263 | 0.20 | 2.0 | 6 | NKD |
| 10527+0029 | HIP 53175AB | 1.65 | 3.0 | 4 | NKD |
| 10527+0029 | HIP 53175BC | 0.17 | 1.2 | 4 | NKD |
| 11100−1017 | HIP 54569AB | 0.37 | 3.1 | 4 | NKD |
| 11100−1017 | HIP 54569Aa,Ab | 0.04 | 0.1 | 4 | NKD |
| 11358+2437 | HIP 56570 | 0.39 | 3.4 | 2 | NKD |
| 11418+0508 | HIP 57058 | 0.06 | 0.0 | 7 | NKD |
| 11563+1102 | SKF 256Aa,Ab | 0.89 | 4.2 | 2 | NKD |
| 12104−4352 | HD 105750 | 0.06 | 1.3 | 13 | Pan |
| 12356−3454 | GJ 1161B | 0.33 | 0.1 | 7 | Pan |
| 13344−2730 | HIP 66229 | 0.04 | 1.5 | 3 | NKD |
| 14106−2826 | HIP 69249 | 0.24 | 2.6 | 4 | NKD |
| 14232−6302 | FIN 221Aa,Ab | 0.10 | 2.2 | 1 | TESS |
| 15003+0739 | HIP 73424 | 0.18 | 4.6 | 1? | REF |
| 15481−5811 | SKF2839Aa,Ab | 0.26 | 1.5 | 5 | Pan |
| 16238−0258 | HIP 80315 | 0.20 | 3.8 | 2 | NKD |
| 17190−4638 | HD 156274B | 0.04 | 1.9 | 8 | Pan |
| 17331−3035 | CHM 6BC | 3.09 | 5.0 | 2 | NKD |
| 18185−3441 | HIP 89708 | 0.18 | 3.5 | 1 | REF |
| 19443−2657 | HD 186265 | 1.06 | 5.0 | 5 | Pan |
| 20118−3825 | RTW2011AB | 4.23 | 0.1 | 1 | NKD |
| 22412−1625 | RTW2241AB | 4.48 | 0.1 | 1 | NKD |
| 22590−0432 | BD−05 5901 | 0.42 | 1.2 | 1 | MSC |
| 23231−7747 | UC 4934Aa,Ab | 0.12 | 0.4 | 1 | HIP |
| 23343+0932 | HIP 116334 | 0.37 | 3.7 | 4 | NKD |

**Note.**
[a] HIP—Hipparcos suspected binary; NKD—nearby K dwarfs; MSC—multiple system; Pan—program by B. Pantoja; REF–reference star; TESS—TESS follow-up; WDS—neglected pair.

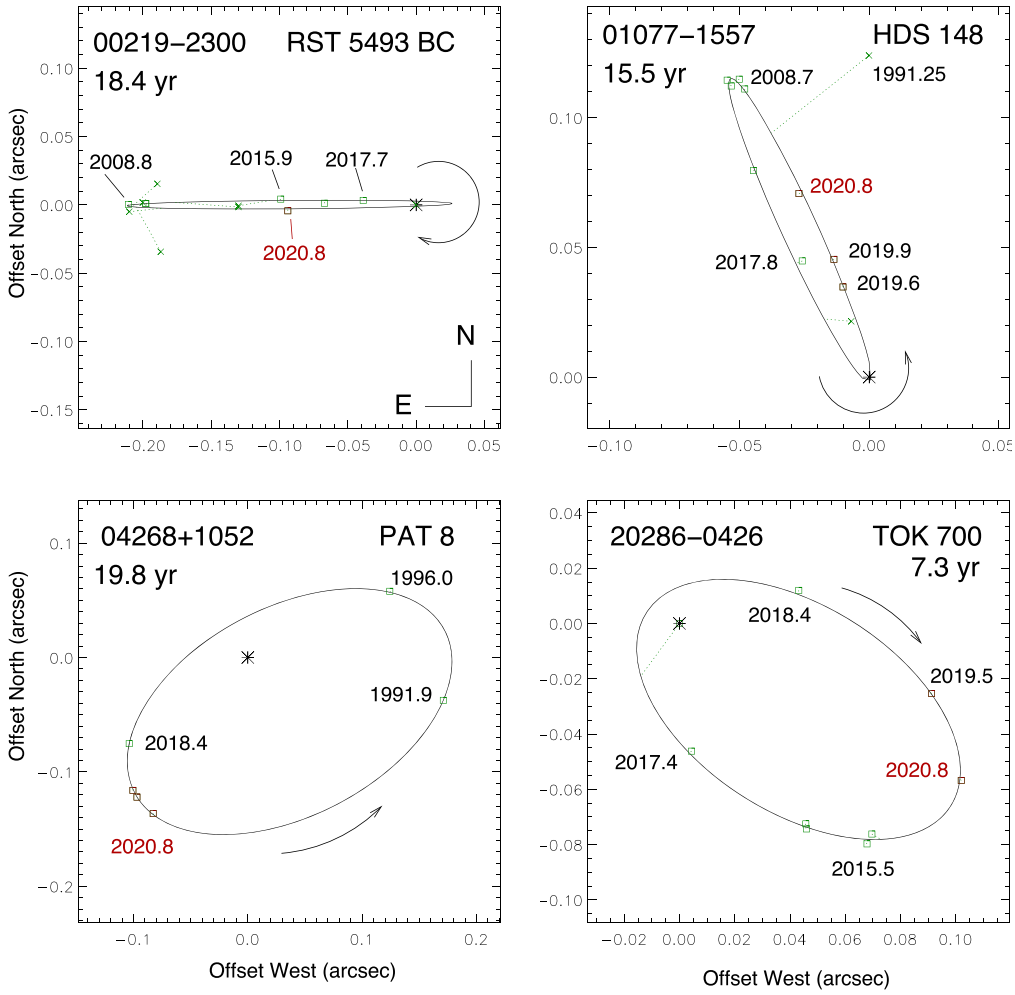


**Figure 3.** Four first-time orbits computed using the SOAR observations in 2020. Accurate speckle measurements are plotted as squares (in red after 2019.0) and visual micrometer measurements are plotted as crosses. The axis scale is in arcseconds.

are real physical binaries, and a few appear to be optical (chance projections).

### *3.4. New and Updated Orbits*

New positional measurements furnished by the SOAR speckle program provide material for calculation of new visual orbits and improvement of the known ones. The previous paper of this series (Tokovinin et al. 2020) gave a long list of new orbits. Here we only give references on the latest orbits resulting from this program (Tokovinin & Latham 2020; Mendez et al. 2021; Tokovinin 2021a, 2021b) and provide examples in Figures 3 and 4. The orbital elements are published, so there is no need to repeat them here. We comment on each pair below.

00219−2300 (ADS 302, HIP 1732) is a triple system at 60 pc from the Sun. The pair BC is located at $6\farcs1$ from the main star *A* and composed of similar K-type dwarfs. Five micrometric measures made since its discovery by S. Rossiter in 1949 were insufficient for orbit calculation, and we see why: the orbit is oriented edge-on and has a large eccentricity $e = 0.83$. The pair was monitored at SOAR since 2008; it closed down and opened again this year after passing through the periastron. The mass sum is $1.5\,\mathcal{M}_{\odot}$.

01077−1557 (HIP 5295) is a pair of solar-type dwarfs discovered by Hipparcos. Its first 15.5 yr orbit is based exclusively on the 10 SOAR measures because the Hipparcos measurement appears to be misleadingly inaccurate. We observed the pair in 2008 near maximum separation; it passed through the periastron of eccentric ($e = 0.98$) orbit in 2019.1 (an uncertain measure was attempted in 2018 below the diffraction limit) and became resolved again in 2019. Although this is a first-time orbit, its elements are quite accurate.

04268+1052 (HIP 20751) is a K0V binary dwarf in the Hyades. Only two measurements were available before 2018, when the SOAR observations started as part of the K-dwarf survey. The arc observed at SOAR is quite short, but, combined with the historic measurements, it allows the calculation of the first 20 yr orbit. The periastron in 2017.4 was, unfortunately, missed, and now the pair is on a slow segment of its orbit. The fit of the seven orbital elements to the six position measurements is nearly perfect (residuals less than 1 mas).

20286−0426 (HIP 100988) is another pair of solar-type stars discovered at SOAR in 2015.5. Its monitoring to date allows calculation of the first 7.3 yr orbit, now almost completely covered.

These four pairs chosen to illustrate new orbits have something in common. They are composed of low-mass stars and their orbits have substantial eccentricities, from 0.65 to 0.98. Radial velocity (RV) monitoring near the periastron can furnish direct measurements of the mass ratios and orbital

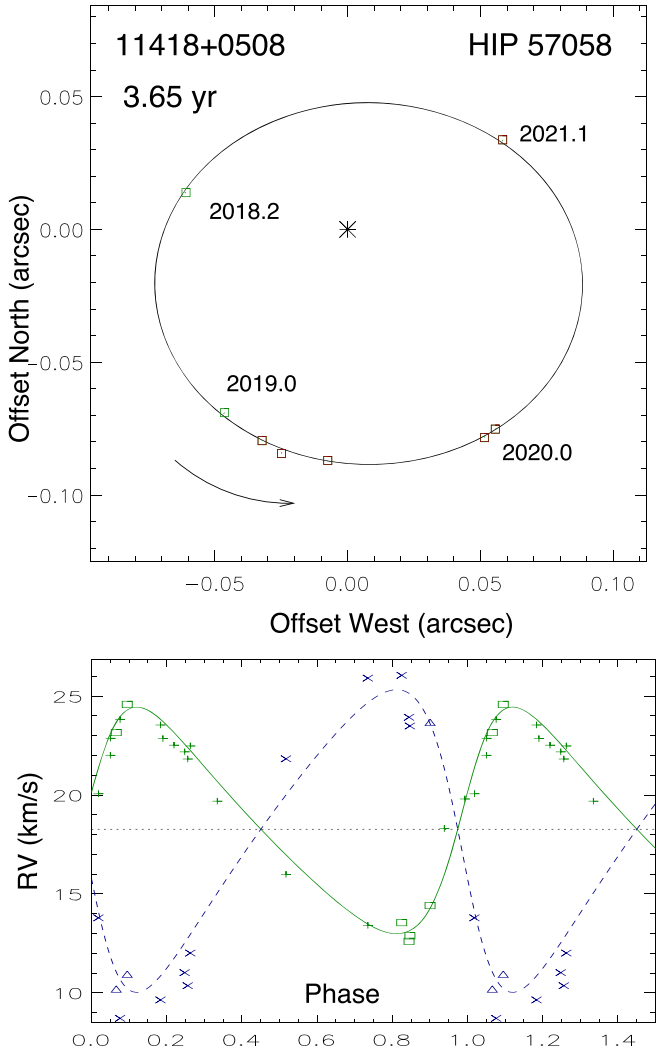


**Figure 4.** Orbit of HIP 57058 in the plane of the sky (top) and its RV curve (bottom).

parallaxes. Such observations can be planned in the future, knowing the visual elements. One notes that the 11 yr duration of the extended Gaia mission is not long enough to derive astrometric orbits from the photocenter motion, while these pairs are too close for a direct resolution by Gaia. However, future combination of speckle orbits and Gaia astrometry will allow accurate modeling of the photocenter motion, leading to unbiased measurements of the parallaxes and, hence, masses.

Figure 4 illustrates the synergy between interferometric and spectroscopic data for the case of a nearby K4V dwarf HIP 57058 (GJ 435.1, distance 31 pc). It was previously identified as a double-lined spectroscopic binary. A preliminary spectroscopic orbit with a period of 725.9 days (2.00 yr) was published by Sperauskas et al. (2019), who also mention its first resolution at SOAR in 2018.2. The pair was also resolved in 2016 by T. Henry, but this measurement is not yet published. Continued monitoring at SOAR revealed that the observed motion is not compatible with the 2 yr period, and the true period is two times longer. Stars $A$ and $B$ are similar ($\Delta I = 0.3$ mag), and a wrong attribution of radial velocities (RVs) to a particular component was the reason for the incorrect spectroscopic orbit (which is single-lined despite the double-lined nature of the system). The

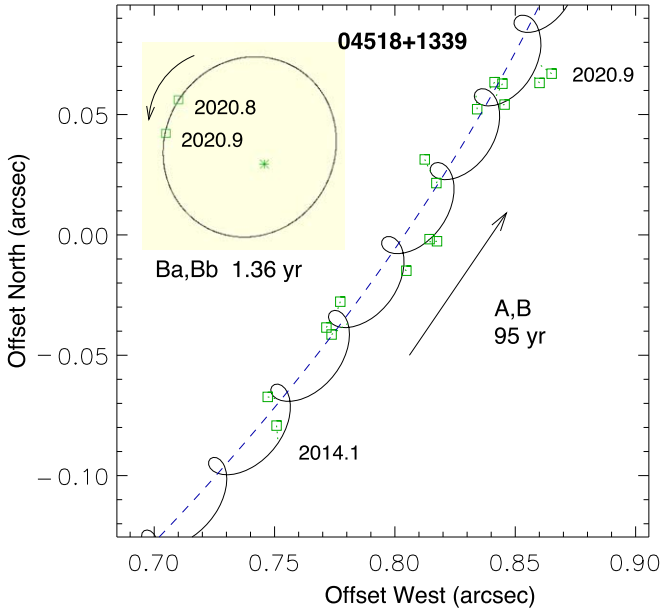


**Figure 5.** Wavy motion of the visual binary J04518+1339 (BU 552) caused by the subsystem Ba,Bb, and the orbit of Ba,Bb (insert) deduced from the RVs and two measures at SOAR.

new orbit with $P = 3.65$ yr presented in Figure 4 uses only RVs of both components when they were resolved spectroscopically. The RV curves look noisy, but, considering the small amplitudes (5.7 and 7.7 km s$^{-1}$) and the difficulty of measuring blended spectra, barely resolved only near the RV maximum, the rms residuals of 0.4 and 1.2 km s$^{-1}$ appear quite acceptable. The residuals of the interferometric measures are small, under 1 mas. The mass sum of 1.35 $\mathcal{M}_\odot$ computed from the orbit and the Gaia parallax matches the RV amplitudes and the spectral type.

### 3.5. Hierarchical Systems

Accumulation of accurate speckle measures with dense coverage made at SOAR allows the study of relative motions in hierarchical stellar systems. The latest papers in this area were already cited (Tokovinin & Latham 2020; Tokovinin 2020, 2021a). Here two additional examples are given.

J04518+1339 (HD 30869, HIP 22607) is a quadruple system belonging to the Hyades cluster. The outer visual pair BU 552 has been known since 1877, and its 95 yr orbit is very well defined by observations covering 1.5 revolutions. Components $A$ and $B$ are double-lined spectroscopic binaries with periods of 143.6 and 496.7 days, respectively (Tomkin et al. 2007). The estimated semimajor axis of Ba,Bb is 33 mas, favoring detection of wobble caused by this subsystem, while the astrometric orbit of Aa,Ab with an amplitude of 4.4 mas was computed by Ren & Fu (2013). From 2016 on, this binary was frequently observed at SOAR. In 2020, the slight elongation of the secondary ACF peak was noted and a triple-star model was fitted, tentatively resolving Ba,Bb on two occasions. Similar elongation can be suspected upon examination of previous observations, but it is often concealed by a false elongation due to telescope vibration or a charge-transfer problem; only observations of the highest quality in the filter $y$ allow marginal resolutions of Ba,Bb at phases near its maximum separation. Figure 5 shows the two measures of Ba,Bb that fit nicely the orbit of Tomkin et al. (2007) with

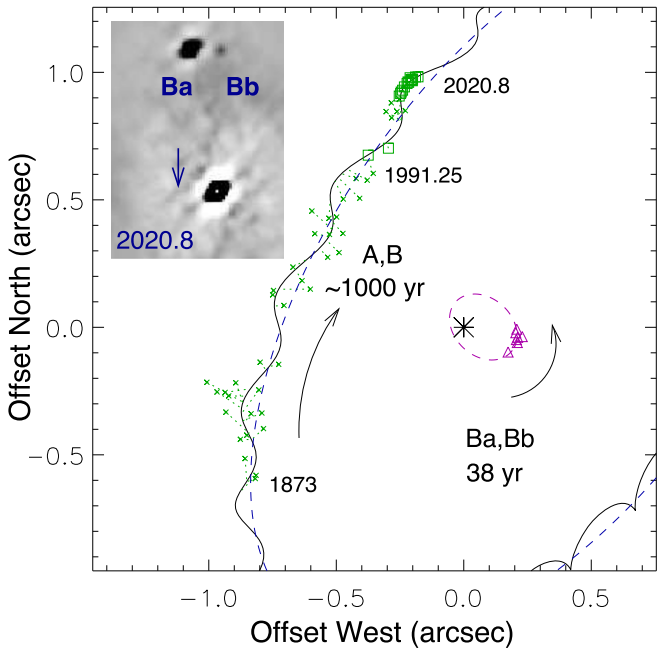


**Figure 6.** Orbital motion of J02460−0457. The wavy line is the motion of A,B with wobble. Squares depict accurate measures from Hipparcos and speckle, crosses are micrometer measures. The inner orbit Ba,Bb is plotted around the center on the same scale by magenta ellipse and triangles. The insert shows the speckle ACF recorded in 2020.8 where the blue arrow shows the missing ACF peak (see the text).

additional elements $a = 34$ mas, $\Omega = 326°$, and $i = 32°$. The axis and inclination match their estimates derived from the spectroscopic orbit. Moreover, the wobble in the motion of A,B with a period of 1.36 yr is rather obvious; its amplitude is 9.7 mas. Motion of the photocenter of A with a 143 day period increases the residuals.

Tomkin et al. (2007) estimate orbital inclination of Aa,Ab to be around 49°, suggesting possible coplanarity with the orbit of A,B (inclination 51°). Ren & Fu (2013) found that the nodes of A,B and Aa,Ab have similar position angles, but they give a mismatching inclination of 94°.4 for Aa,Ab. Our work establishes the orientation of the orbit of Ba,Bb: it is inclined to the orbit of A,B by 26°. These preliminary results should be refined by further observations, preferably with larger aperture (the resolution of Ba,Bb at SOAR is just marginal).

J02460−0457 (HD 17251, HIP 12912) is a triple system where the outer pair A,B (BU 83) has been known since 1873. A third faint component was discovered at SOAR in 2016 and attributed to the primary (Tokovinin et al. 2018), based on the sign of the wobble. Continued observations show that this is not correct and the faint companion in fact belongs to the secondary star *B*. The situation is illustrated in Figure 6. Generally, the ACF of a triple star contains six secondary peaks corresponding to six vectors between its components. The relative intensity of the peaks is proportional to the products of the relative fluxes; the two weakest peaks that correspond to the pair of the faintest stars often are lost in the noise, as is the case here. The arrow shows the position of the missing peak corresponding to the faint companion. If it were associated with A, this missing peak would be stronger than the well-visible peak Bb. The missing peak was marginally seen in the discovery ACF, prompting the original wrong attribution of the new companion.

The rotation direction of the Ba,Bb pair is opposite to A,B. Existing data were reprocessed with the assumption that the companion is associated with B, resulting in more accurate measurements of the Ba,Bb positions. The wave in the A,B motion does not depend on the choice, so the original argument associating the companion with A was not valid. If the new companion were associated with A, the wobble should produce a proper motion (PM) anomaly (difference between the Gaia short-term PM and the long-term PM of the photocenter) of about 2 mas yr$^{-1}$, oriented in the decl. direction. The measured PM anomaly in decl. is $0.15 \pm 0.14$ mas yr$^{-1}$, compatible with zero; it proves that the subsystem is associated with component *B*.

The inner and outer orbits fitted to the available measures, shown in Figure 6, are still preliminary. The opposite sense of rotation excludes their coplanarity: the mutual inclination is either 130° or 95°. Unequal masses and misaligned, eccentric orbits are signs of dynamical interactions that probably defined the architecture of this triple system.

## 4. Summary

The total number of observations made with HRCam to date is about 25,000. This paper documents the observations made in 2020, as well as earlier unpublished data. The HRCam at SOAR is used by various programs, executed in a concerted and optimized way and complemented by the uniform data reduction and calibration procedures. Focused initially on the determination of visual orbits, the programs expanded into surveys of binarity in various populations. Still, the orbits of both previously known pairs and those discovered at SOAR remain the major use of the HRCam data.

This paper presents results of the large survey of the YMG population and of the K-type dwarfs in the solar neighborhood. Both programs discovered a substantial number of tight pairs with fast orbital motion. Their continued monitoring will lead to orbit calculation and measurements of masses in the near future. For example, the first orbit of the K-dwarf HIP 57058 presented above uses 2 yr of SOAR data in combination with the longer RV coverage. Several orbits of new M-dwarf pairs with short periods will be published by E. Vrijmoet et al. (2021, in preparation).

Flexibility of the HRCam observing procedure brings unexpected benefits. When the unusual sextuple eclipsing system TIC 168789840 (J04141−3155) was discovered, it could be quickly tested at SOAR and resolved into a 0″.4 pair —a key piece of information for unveiling the architecture of this unique object (Powell et al. 2021). Thus, the ongoing SOAR speckle program is a backbone for testing future discoveries in a quick and efficient way.

We thank the SOAR operators for efficient support of this program, and the SOAR director J. Elias for allocating some technical time. This work is based in part on observations carried out under CNTAC programs CN2019A-2, CN2019B-13, CN2020A-19, and CN2020B-10.

R.A.M. and E.C. acknowledge support from the FONDECYT/CONICYT grant # 1190038. T.H. appreciates support of this work through NSF grants AST-1517413 and AST-1910130.

This work used the SIMBAD service operated by Centre des Données Stellaires (Strasbourg, France), bibliographic references from the Astrophysics Data System maintained by SAO/NASA, and the Washington Double Star Catalog maintained at USNO. This work has made use of data from the European

Space Agency (ESA) mission Gaia (https://www.cosmos.esa.int/gaia) processed by the Gaia Data Processing and Analysis Consortium (DPAC, https://www.cosmos.esa.int/web/gaia/dpac/consortium). Funding for DPAC has been provided by national institutions, in particular the institutions participating in the Gaia Multilateral Agreement.

*Facility:* SOAR

## ORCID iDs

Andrei Tokovinin https://orcid.org/0000-0002-2084-0782
Brian D. Mason https://orcid.org/0000-0003-4824-0938
Rene A. Mendez https://orcid.org/0000-0003-1454-0596
Andrew W. Mann https://orcid.org/0000-0003-3654-1602
Todd J. Henry https://orcid.org/0000-0002-9061-2865

## References

Gaia Collaboration, Brown, A. G. A., Vallenari, A., et al. 2018, A&A, 616, A1
Gagné, J., Mamajek, E. E., Malo, L., et al. 2018, ApJ, 856, 23
Hartkopf, W. I., Mason, B. D., & Worley, C. E. 2001, AJ, 122, 3472
Hartkopf, W. I., Tokovinin, A., & Mason, B. D. 2012, AJ, 143, 42
Horch, E. I., Tokovinin, A., Weiss, S. A., et al. 2019, AJ, 157, 56
Horch, E. P., Casetti-Dinescu, D. I., Camarata, M. A., et al. 2017, AJ, 153, 212
Horch, E. P., van Belle, G. T., Davidson, J. W., Jr., et al. 2015, AJ, 150, 151
Mason, B. D., Wycoff, G. L., Hartkopf, W. I., et al. 2001, AJ, 122, 3466, (WDS)
Mendez, R. A., Clavería, R. M., & Costa, E. 2021, AJ, 161, 155
Mendez, R. A., Claveria, R. M., Orchard, M. E., & Silva, J. F. 2017, AJ, 154, 187
Newton, E. R., Mann, A. W., Tofflemire, B. M., et al. 2019, ApJL, 880, L17
Pantoja, B. M., Jenkins, J. S., Girard, J. H., et al. 2018, MNRAS, 479, 4958
Powell, B. P., Kostov, V., Rappaport, S. A., et al. 2021, AJ, 161, 162
Ren, S., & Fu, Y. 2013, AJ, 145, 81
Rizzuto, A. C., Ireland, M. J., & Kraus, A. L. 2015, MNRAS, 448, 2737
Sperauskas, J., Deveikis, V., & Tokovinin, A. 2019, A&A, 626, 31
Stassun, K. G., Oelkers, R. J., Paegert, M., et al. 2019, AL, 158, 138
Tokovinin, A. 2012, AJ, 144, 56
Tokovinin, A. 2018, PASP, 130, 5002
Tokovinin, A. 2020, AstL, 46, 612
Tokovinin, A. 2021a, AJ, 161, 144
Tokovinin, A. 2021b, Inf. Circ., 203, 1
Tokovinin, A., & Briceño, C. 2020, AJ, 15, 159
Tokovinin, A., Cantarutti, R., Tighe, R., et al. 2010b, PASP, 122, 1483
Tokovinin, A., & Latham, D. W. 2020, AJ, 160, 251
Tokovinin, A., Mason, B. D., & Hartkopf, W. I. 2010a, AJ, 139, 743
Tokovinin, A., Mason, B. D., & Hartkopf, W. I. 2014, AJ, 147, 123
Tokovinin, A., Mason, B. D., Hartkopf, W. I., et al. 2015, AJ, 150, 50
Tokovinin, A., Mason, B. D., Hartkopf, W. I., et al. 2016, AJ, 152, 116
Tokovinin, A., Mason, B. D., Hartkopf, W. I., et al. 2018, AJ, 155, 235
Tokovinin, A., Mason, B. D., Mendez, R. A., et al. 2019, AJ, 158, 148
Tokovinin, A., Mason, B. D., Mendez, R. A., et al. 2020, AJ, 160, 7
Tomkin, J., Griffin, R. F., & Alzner, A. 2007, Obs, 127, 87
Toonen, S., Portegies Zwart, S., Hanera, A. S., & Bandopadhyay, D. 2020, A&A, 640, 16
Zari, E., Hashemi, H., Brown, A. G. A., Jardine, K., & de Zeeuw, P. T. 2018, A&A, 620, A172
Ziegler, C., Tokovinin, A., Briceño, C., et al. 2020, AJ, 159, 19
Ziegler, C., Tokovinin, A., Latiolais, M., et al. 2021, AJ, submitted